Journal of Electronics, Electromedical Engineering, and Medical Informatics
Homepage: jeeemi.org; Vol. 8, No. 2, April 2026, pp: 751-768 e-ISSN: 2656-8632

RESEARCH PAPER OPEN ACCES

Comparative Evaluation of LSTM and Metaheuristic-Optimized Neural Networks for ECG Prediction under Limited Data Conditions

Giovanni Dimas Prenata[1], Ahmad Ridho'i[1], Mohd Rizal Arshad[2]

[1] Faculty of Intelligent Electrical and Informatics Technology, Universitas 17 Agustus 1945 Surabaya, Surabaya, Indonesia

[2] School of Robotics, Xi'an Jiaotong-Liverpool University (XJTLU), Taicang, China

Corresponding author: Giovanni Dimas Prenata. (e-mail: gprenata@untag-sby.ac.id), **Author(s) Email**: Ahmad Ridhoi (e-mail: ridhoi@untag-sby.ac.id, Mohd Rizal Arshad (e-mail: IRE@xjtlu.edu.cn)

Abstract This study presents a comparative evaluation of Deep Feedforward Neural Network (DFFNN) models optimized using single-stage metaheuristic approaches, including Genetic Algorithm (GA), Particle Swarm Optimization (PSO), and Grey Wolf Optimization (GWO), as well as a multi-stage hybrid optimization strategy (GA+GWO) for ECG-based emotion classification. The experimental dataset consists of ECG recordings collected from three elderly participants using a Sparkfun AD8232 sensor under controlled emotional stimuli, representing a limited-subject and small-data scenario. Feature extraction is conducted using Heart Rate Variability (HRV) parameters derived from both time domain (Mean RR, SDNN, RMSSD, Mean HR, and STD HR) and frequency domain (LF, HF, and LF/HF ratio). Experimental results from six repeated trials demonstrate that the multi-stage DFFNN+GA+GWO model achieves the best optimization performance, yielding the lowest Mean Squared Error (MSE) of 0.01599 and a consistent training accuracy of up to 85.71%. Compared with single-stage optimization methods, the hybrid approach exhibits improved convergence behavior and reduced performance variance, indicating enhanced optimization stability. However, test accuracy remains relatively limited (33.33%–50.00%), reflecting constrained generalization capability due to the small dataset and the absence of subject-wise or external validation. Further statistical analysis using confidence intervals and nonparametric testing confirms that the observed performance improvements are primarily associated with optimization stability rather than statistically significant gains in predictive generalization. Therefore, this study emphasizes the role of metaheuristic optimization in stabilizing neural network training under limited data conditions. The findings should be interpreted as a pilot feasibility study, and future work is required to validate the proposed approach using larger, more diverse datasets and more rigorous validation strategies.

Keywords Electrocardiogram; Long Short-Term Memory; Genetic Algorithm; Deep Feedforward Neural Network; Grey Wolf Optimization; Backpropagation Through Time.

I. Introduction

Electrocardiogram (ECG) signals are fundamental for assessing cardiac electrical activity and play a central role in early diagnosis and real-time clinical monitoring. However, ECG prediction remains a challenging task because the signal is nonlinear, non-stationary, and highly sensitive to noise difficulties that become more prominent when datasets are limited, as commonly observed in small-scale biomedical studies. Recent advances in deep learning have significantly improved the analysis of sequential biomedical data, with Long Short-Term Memory (LSTM) networks emerging as a leading model due to their ability to capture long-range temporal dependencies. Jiang et al. demonstrated that LSTM-based architectures can effectively learn temporal variations in cardiac cycles, though their performance depends heavily on large annotated datasets and considerable computational resources, which restricts deployment in real-time or resource-limited environments [1]. Similarly, Yildirim et al. reported that CNN–LSTM hybrids achieve high arrhythmia classification accuracy, yet their implementation remained focused on classification rather than waveform prediction and required extensive datasets for optimal performance [2]. Additional studies, such as the CWT–CNN method explored by Wang et al., confirmed strong classification capabilities but did not extend to regression-based ECG forecasting [3]. Indonesian research by Prihatmoko et al. further revealed that the Wavelet Transform combined with backpropagation neural networks could extract ECG features effectively but was sensitive to noise and exhibited weaker generalization when training data were limited [4]. Complementary work by Kanwal et al. integrated Wavelet Packet Transform with entropy-based features, improving feature robustness but still relying on handcrafted extraction rather than end-to-end prediction models [5]. Beyond deep learning methods, metaheuristic optimization has gained increasing traction for enhancing neural network performance. Holland's foundational analysis of Genetic Algorithms (GAs) highlighted their strength in global search and robustness against local minima, making them suitable

Manuscript received 8 August 2025; Revised 20 February 2026; Accepted 20 March 2026; Available online 23 April 2026
Digital Object Identifier (**DOI**): https://doi.org/10.35882/jeeemi.v8i2.1524

for optimizing neural network parameters in environments with gradient instability [6]. The Grey Wolf Optimizer (GWO), introduced by Mirjalili et al., demonstrated competitive performance across numerous engineering optimization benchmarks owing to its effective balance between exploration and exploitation [7]. In Indonesia, Warsito applied GA for health-related predictive modeling and reported encouraging performance on limited datasets, further supporting the relevance of evolutionary optimization for biomedical applications [8]. More recently, Li et al. proposed an Improved GWO (IGWO) for short-term forecasting of crude oil prices and achieved superior accuracy and convergence stability compared to conventional evolutionary algorithms, underscoring the potential of GWO-based approaches for time-series prediction tasks [9].

Despite these advancements, existing research presents three major limitations. First, most deep learning studies focus primarily on ECG classification rather than continuous waveform forecasting, leaving regression-based prediction models underexplored. Second, although metaheuristic algorithms such as GA and GWO have demonstrated promising optimization capabilities, their application for ECG waveform prediction, particularly under small-data biomedical conditions, remains limited. In this work, the term small-data biomedical condition refers to ECG recordings collected from only three elderly participants, with each session lasting approximately 2-3 minutes at a 250 Hz sampling rate, resulting in limited subject diversity despite having thousands of time samples. Third, prior literature lacks a comparative evaluation of gradient-based LSTM models and metaheuristic-driven neural architectures such as GA-optimized LSTM and GWO-trained DFFNN, creating a clear gap in understanding their relative performance, convergence behavior, and generalization capability. These gaps are addressed by comparing (i) a gradient-based sequential model (LSTM), (ii) a metaheuristic-optimized recurrent model (LSTM–GA), and (iii) a metaheuristic-optimized lightweight feedforward model (DFFNN–GWO), enabling analysis of accuracy, robustness across repeated runs, and convergence behavior under limited-subject ECG data.

In this study, the DFFNN used in the hybrid model follows a compact structure of 6 input neurons with three hidden layers (2-2-2) and one output neuron (1) using sigmoid activation, designed to maintain a lightweight computation footprint. To address these gaps, this study presents a comprehensive comparison of three predictive modeling frameworks for ECG time-series forecasting: (1) a baseline LSTM model trained using a simplified gradient-based strategy on the output layer, (2) a hybrid LSTM–GA model that applies Genetic Algorithm optimization to tune key gate parameters without relying on full backpropagation, and (3) a DFFNN–GWO model in which network weights are optimized through the Grey Wolf Optimizer. By evaluating these architectures under a limited-data ECG setting collected from elderly participants, this study provides new insights into computationally efficient and robust approaches for biomedical signal prediction, supporting the development of lightweight cardiac monitoring and decision-support systems.

This study presents a comparative analysis of Deep Feedforward Neural Network (DFFNN) models optimized using single-stage (Genetic Algorithm, Particle Swarm Optimization, Grey Wolf Optimization) and multi-stage (GA+GWO) metaheuristic approaches for ECG-based emotion classification. The dataset consists of ECG recordings obtained from three elderly participants using a Sparkfun AD8232 sensor in response to controlled emotional stimuli, resulting in a limited-subject experimental setting. Feature extraction is performed using time-domain (Mean RR, SDNN, RMSSD, Mean HR, STD HR) and frequency-domain (LF, HF, LF/HF) Heart Rate Variability (HRV) parameters.

Experimental results from six repeated trials show that the proposed multi-stage DFFNN+GA+GWO achieves the lowest Mean Squared Error (MSE) of 0.01599 and maintains a consistent training accuracy of up to 85.71%, outperforming single-stage optimization methods. However, test accuracy remains limited (33.33%–50.00%), indicating constraints in generalization due to the small dataset and the absence of subject-wise validation. Statistical analysis using confidence intervals and nonparametric testing further supports that performance improvements are associated with optimization stability rather than significant generalization gains. This study highlights that metaheuristic optimization plays a critical role in stabilizing neural network training under small-data conditions. Nevertheless, the findings are specific to the constrained experimental setup and should be validated on larger and more diverse datasets in future work.

In addition to signal-processing challenges, ECG signals are strongly influenced by emotional and physiological states. Psychological and physiological studies have shown that emotional conditions such as stress, sadness, and arousal directly affect autonomic nervous system activity, which is reflected in ECG dynamics and HRV characteristics [26], [27], [28]. These findings highlight the importance of incorporating emotion-related variability into ECG-based predictive modeling. Recent studies have further explored hybrid and optimization-based approaches for ECG analysis, combining machine learning models with advanced optimization strategies to improve predictive performance and robustness [32], [33], [34]. These approaches demonstrate the growing interest in integrating metaheuristic techniques with neural architectures, particularly in biomedical signal processing applications.

II. Literature and Method

The dataset used in this study was collected from three elderly participants using a Sparkfun AD8232 ECG sensor connected to an Arduino Uno R3. Each participant was exposed to emotional stimulus videos representing three emotional states: sadness, surprise, and anger. To minimize emotional carryover effects,

Manuscript received 8 August 2025; Revised 20 February 2026; Accepted 20 March 2026; Available online 23 April 2026
Digital Object Identifier (**DOI**): https://doi.org/10.35882/jeeemi.v8i2.1524

relaxation videos were presented between stimuli to return participants to a neutral state. The recorded ECG signals were stored in CSV format for further processing. A total of 27 samples were obtained, consisting of 21 training samples and 6 testing samples. Due to the limited number of participants, the dataset does not include subject-wise separation, and the experimental design follows a within-subject evaluation approach. This limitation is explicitly acknowledged and considered in the interpretation of results.

All experiments were conducted using fixed random seeds to ensure reproducibility. Initialization ranges for weights and biases were uniformly sampled within [-0.5, 0.5]. The stopping criteria for metaheuristic optimization were defined by a maximum number of iterations without early stopping.

A. Theoretical Background

1. Electrocardiogram (ECG) Signals

ECG signal analysis often relies on morphological and temporal features such as PQRST intervals, which are widely used for distinguishing physiological and pathological conditions [29]. In addition, feature extraction techniques based on ECG waveform segmentation and interval analysis remain fundamental in both classical and machine learning-based approaches [30].

An Electrocardiogram (ECG) is a biomedical signal that records the heart's electrical activity using electrodes placed on the body surface. The signal typically consists of the P wave, the QRS complex, and the T wave. The P wave reflects atrial depolarization, the QRS complex represents ventricular depolarization, and the T wave corresponds to ventricular repolarization [10] [11]. From a mathematical perspective, ECG signals are often modeled as the superposition of Gaussian functions:

$$ECG(t) \approx \sum_{i=1}^{n} A_i \cdot \exp\left(-\frac{(t-\mu_i)^2}{2\sigma_i^2}\right) \quad (1)$$

where *ECG(t)* denotes the modeled ECG amplitude at time *t*; A_i is the amplitude contribution of the i-th Gaussian basis; μ_i represents the center of the Gaussian function; σ_i is its standard deviation; and *N* is the number of Gaussian components utilized.

The ECG waveform approximation is mathematically modeled using a Gaussian-based formulation, as presented in Eq. (1), which enables synthetic representation of PQRST morphology for analytical and machine learning purposes.

Where Ai is the amplitude of each component, μi is the center time of the component, and σi represents the width or duration of the component. This empirical formulation facilitates the generation of synthetic PQRST signals and feature analysis for arrhythmia diagnosis as well as AI-based biomedical signal research [12].

2. Long Short-Term Memory (LSTM)

Recurrent Neural Networks (RNNs) suffer from the vanishing gradient problem when handling long sequential data. To address this, Hochreiter and Schmidhuber introduced the Long Short-Term Memory (LSTM) architecture [1].

LSTM networks consist of three main gates:

1. Forget gate (f_t): determines which information is discarded.
2. Input gate (i_t): determines which new information is added to the cell state.
3. Output gate (o_t): determines which information is output.

The internal mechanics of the LSTM unit, including the forget, input, candidate, and output gates, along with cell and hidden state updates, are expressed in Eqs. (2)–(7). These Eq. s define how temporal information is retained, discarded, and transformed across time steps. The governing Eq. s are [13]:

$$f_t = \sigma\,(W_f \cdot |h_{t-1}, X_t| + b_f) \quad (2)$$

$$i_t = \sigma\,(W_f \cdot |h_{t-1}, X_t| + b_i) \quad (3)$$

$$\tilde{C}_t = \tanh(W_c \cdot |h_{t-1}, X_t| + b_c) \quad (4)$$

$$C_t = f_t \odot C_{t-1} + i_t \odot \tilde{C}_t \quad (5)$$

$$O_t = \sigma\,(W_o \cdot |h_{t-1}, X_t| + b_o) \quad (6)$$

$$h_t = o_t \odot \tanh(C_t) \quad (7)$$

Where C_t is the cell state, *ht* is the hidden state, σ sigmaσ is the sigmoid function, and tanh is the hyperbolic tangent activation. LSTM has proven effective for biomedical signal prediction (e.g., ECG) because it can capture long-term temporal patterns [14] [15] [16].

The mathematical formulation of the Long Short-Term Memory (LSTM) unit used in this study is expressed through Eqs. (2)–(7). Each Eq. governs a specific gating mechanism that regulates how information is stored, updated, and propagated across time steps. The parameters of each Eq. are described in detail as follows.

Eqs. (2) defines the forget gate f_t, which determines the proportion of the previous cell state C_{t-1} that should be retained. The term W_f represents the weight matrix associated with the forget gate, b_f denotes the bias vector, and $[h_{t-1} ; x_t]$ is the concatenation of the previous hidden state and the current input. The sigmoid activation function *σ*(.) ensures that the output of the forget gate lies between 0 and 1, allowing the model to selectively discard irrelevant information. Eq. (3) describes the input gate i_t, which regulates the amount of new information that enters the cell state. Similar to the forget gate, W_i is the input gate weight matrix, bib_ibi is the corresponding bias vector, and *σ*(.) is the sigmoid activation. The input gate works jointly with the candidate memory vector to update the cell state. Eq. (4) computes the candidate memory vector $\tilde{C}_t$, which represents the new information proposed to be added to the cell state. The matrix W_c and bias b_c control the transformation of the concatenated input $[h_{t-1} ; x_t]$. The hyperbolic tangent activation function tanh(.) maps the candidate memory values to the range [−1,1], enabling both positive and negative contributions to the cell state. Eq. (5) updates the cell state C_t by combining the retained memory from the previous time step and the newly generated candidate memory. The symbol ⊙ denotes element-wise (Hadamard) multiplication. The term $f_t \odot C_{t-1}$ represents the preserved portion of the old memory, while $i_t \odot \tilde{C}_t$ adds relevant new information selected by the input gate.

Manuscript received 8 August 2025; Revised 20 February 2026; Accepted 20 March 2026; Available online 23 April 2026
Digital Object Identifier (**DOI**): https://doi.org/10.35882/jeeemi.v8i2.1524

Eq. (6) defines the output gate O_t, which controls how much of the updated cell state is exposed to the next hidden state. The parameters W_o and b_o correspond to the weight matrix and bias vector of the output gate. The sigmoid activation determines which parts of the internal memory are allowed to influence the network output. Eq. (7) produces the new hidden state h_t, which serves as the LSTM's main output at time step *t*. It is computed by modulating the activated cell state tanh(C_t) with the output gate o_t through element-wise multiplication. This mechanism allows the LSTM to control both the amount and the form of information that is passed forward in time. Together, Eqs. (2)–(7) describe the complete information flow within the LSTM unit, enabling it to learn long-term temporal dependencies from ECG time-series data and effectively capture both short-term variations and long-range dynamics

3. Genetic Algorithm (GA)

Genetic Algorithm (GA) is an evolutionary optimization method introduced by Mitchell [17]. GA mimics natural selection through the processes of population initialization, selection, crossover, and mutation. For neural network optimization, the fitness function is typically defined as the Mean Squared Error (MSE) [18]:

$$MSE = \frac{1}{N}\sum_{i=1}^{N}(y_i - \hat{y}_i)^2 \quad (8a)$$

where y_i is the actual target, $\hat{y}$ is the predicted output, and NNN is the number of samples. GA helps neural networks escape from local minima often encountered in conventional gradient descent methods [19]. Model performance was assessed using the Mean Squared Error metric, as defined in Eq. (8), which measures the average squared difference between actual and predicted values. Crossover is applied to recombine two parent chromosomes *p*1 and p_2 to generate a new offspring solution.

$$child = [p_1(1 : c), p_2(c + 1 : end)\,] \quad (8b)$$

where ccc denotes the crossover point and the offspring inherits the first segment from p_1 and the remaining segment from p_2. To maintain population diversity and avoid premature convergence, mutation introduces small random perturbations to selected genes.

$$x_j \leftarrow x_j + \epsilon, \epsilon \sim \mathrm{U}(-\delta, \delta) \quad (8c)$$

where x_j is the *j*-th gene and δ controls the mutation amplitude. This equation quantifies the average squared difference between the ground-truth values and the predicted outputs generated by each model. In this formulation, *N* denotes the total number of data points in the test set, y_i represents the actual ECG signal value at the *i*-th sample, and $\hat{y}_i$ corresponds to the predicted value produced by the model. The term $(y_i - \hat{y}_i)^2$ captures the squared prediction error for each sample, ensuring that larger deviations are penalized more heavily than smaller ones. The division by *N* normalizes the total squared error, yielding a scale-independent measure that allows fair comparison across multiple models and datasets. As a loss function, MSE is widely used in regression-based prediction tasks, including biomedical time-series forecasting, due to its mathematical simplicity, differentiability, and sensitivity to large errors. In this study, MSE serves as one of the primary evaluation metrics to assess the prediction accuracy of the LSTM, LSTM-GA, DFFNN, and DFFNN-GWO models. Lower MSE values indicate better predictive performance and closer alignment between predicted and actual ECG signals.

4. Grey Wolf Optimizer (GWO)

The Grey Wolf Optimizer (GWO), introduced by Mirjalili [20], is inspired by the cooperative hunting behavior of grey wolves. GWO establishes a hierarchy of α (alpha), β (beta), δ (delta), and ω (omega), where the top three guide the pack toward optimal solutions. The distance computation and intermediate position updates in Grey Wolf Optimizer are formulated in Eqs. (9)–(12), which emulate the hunting strategy of alpha, beta, and delta wolves guiding the search agents. The position update mechanism of the Grey Wolf Optimizer (GWO) used in this study follows the mathematical formulation introduced in [7]. The distance vectors between the current search agent and the three leading wolves Alpha (α), Beta (β), and Delta (δ) are defined in Equations (9) - (11):

$$\overrightarrow{D_\alpha} = \left|\overrightarrow{C_1} \,.\, \overrightarrow{X_\alpha} - \vec{X}(t)\right| \text{[7]} \quad (9)$$

$$\overrightarrow{D_\beta} = \left|\overrightarrow{C_2} \,.\, \overrightarrow{X_\beta} - \vec{X}(t)\right| \text{[7]} \quad (10)$$

$$\overrightarrow{D_\delta} = \left|\overrightarrow{C_3} \,.\, \overrightarrow{X_\delta} - \vec{X}(t)\right| \text{[7]} \quad (11)$$

$$\vec{X}(t+1) = \frac{\overrightarrow{X_1} + \overrightarrow{X_2} + \overrightarrow{X_3}}{3} \text{[7]} \quad (12)$$

Here, $\vec{X}(t)$ denotes the current position of a grey wolf at iteration *t*, while $\overrightarrow{X_\alpha}$α, $\overrightarrow{X_\beta}$, and $\overrightarrow{X_\delta}$ represent the positions of the top three wolves that guide the search process. The coefficient vectors $\overrightarrow{C_1}$, $\overrightarrow{C_2}$, and $\overrightarrow{C_3}$ introduce random perturbations that increase search diversity and help avoid premature convergence. The distance vectors $\overrightarrow{D_\alpha}$, $\overrightarrow{D_\beta}$, and $\overrightarrow{D_\delta}$ quantify how far each search agent is from the three leaders. Based on these distances, three candidate updated positions $\overrightarrow{X_1}$, $\overrightarrow{X_2}$, and $\overrightarrow{X_3}$ are computed using Equations (13) - (15):

$$\overrightarrow{X_1} = \overrightarrow{X_\alpha} - \overrightarrow{A_1} \,.\, \overrightarrow{D_\alpha} \text{[7]} \quad (13)$$

$$\overrightarrow{X_2} = \overrightarrow{X_\beta} - \overrightarrow{A_2} \,.\, \overrightarrow{D_\beta} \text{[7]} \quad (14)$$

$$\overrightarrow{X_3} = \overrightarrow{X_\delta} - \overrightarrow{A_3} \,.\, \overrightarrow{D_\delta} \text{[7]} \quad (15)$$

where $\overrightarrow{A_1}$, $\overrightarrow{A_2}$, and $\overrightarrow{A_3}$ are adaptive coefficient vectors that linearly decrease over iterations. These coefficients control the balance between exploration and exploitation allowing the algorithm to search broadly in early iterations and converge more tightly during later stages.
The final updated position of each grey wolf is computed as the average of these three candidate positions, as shown in Eq. (12). This averaging mechanism enables the search agents to follow the collective guidance of the alpha, beta, and delta wolves, resulting in a more stable and robust convergence behavior. In this study, these formulations are applied to optimize the weights and biases of the DFFNN model, allowing the algorithm to minimize prediction error without relying on gradient-based backpropagation.

Manuscript received 8 August 2025; Revised 20 February 2026; Accepted 20 March 2026; Available online 23 April 2026
Digital Object Identifier (**DOI**): https://doi.org/10.35882/jeeemi.v8i2.1524

Where α decreases linearly from 2 to 0 during iterations to balance exploration and exploitation. GWO has proven effective in optimizing neural network training for biomedical signal prediction [21] [16]. Final position estimation in the GWO algorithm is derived through averaging candidate updates influenced by alpha, beta, and delta wolves, as shown in Eqs. (13)–(15).

Various metaheuristic optimization techniques, including hybrid and multi-stage strategies, have been reported to enhance convergence stability and improve global search capability in neural network training [35], [36], [37]. These methods are particularly advantageous in complex, nonlinear optimization landscapes where gradient-based approaches may struggle.

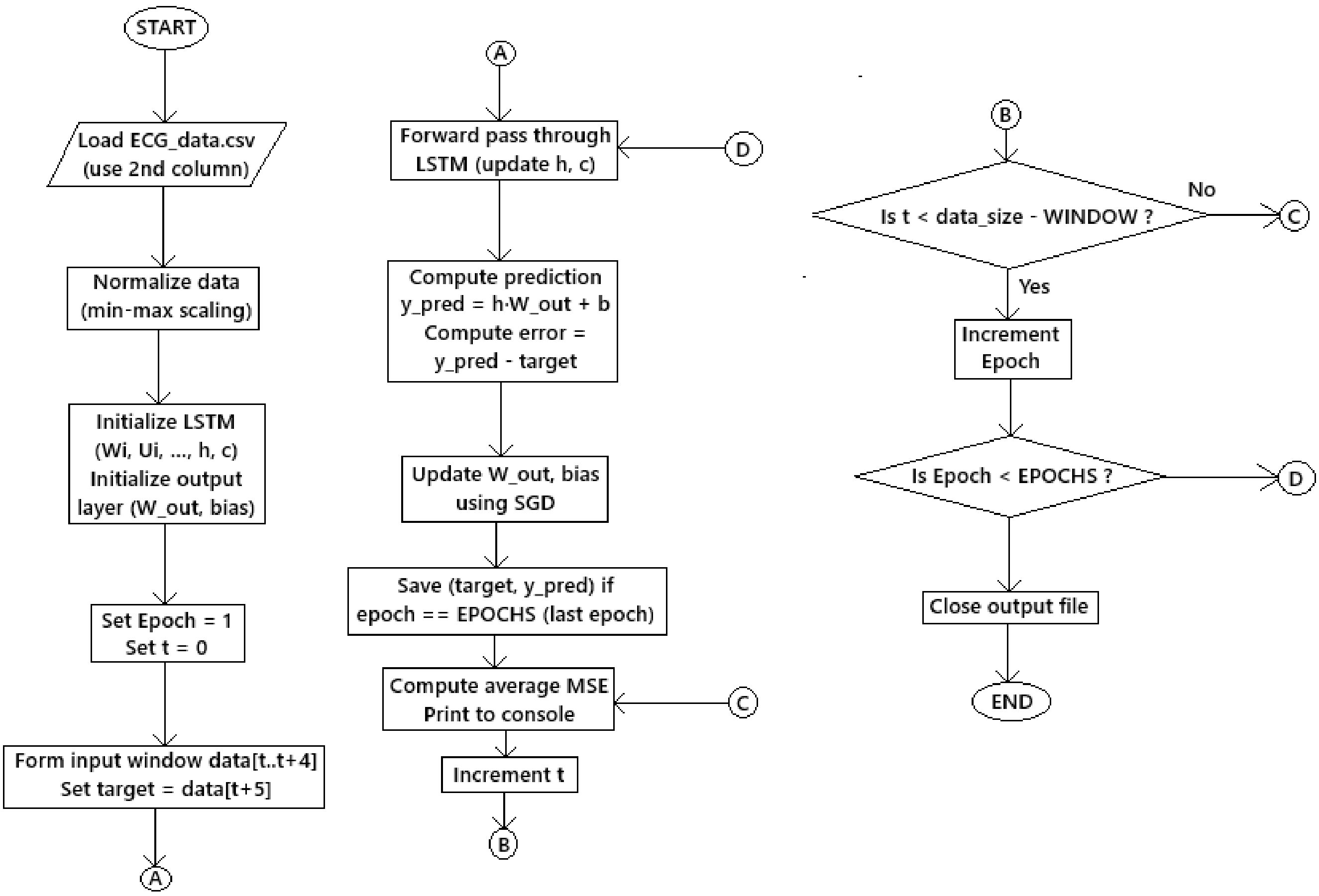

Fig. 1. Detailed flowchart illustrating the complete operational process of the pure LSTM model.

5. LSTM Model

The Long Short-Term Memory (LSTM) model was employed to predict ECG signals by capturing sequential dependencies and long-term temporal patterns inherent in biomedical time-series data. This model addresses the vanishing gradient problem commonly encountered in recurrent neural networks (RNNs) and has been proven effective for handling complex nonlinear signals such as ECG. Fig. 1 illustrates the overall methodological framework of the proposed system. From Fig. 1, stage 1 start with Data Ppreparation. The ECG dataset was normalized into the range [0,1] using min–max scaling to ensure stability during training. A sliding window of five consecutive data points was applied, where each window served as the input and the subsequent sixth value was treated as the prediction target. This approach enabled the model to learn temporal dependencies from recent observations to predict the next signal value.

Stage 2, Model Architecture. The implemented LSTM network consists of a hidden layer with 32 units, each equipped with standard gating mechanisms: the input gate, forget gate, output gate, and candidate memory cell. These gates control the flow of information by selectively retaining or discarding past states. The output of the hidden layer is connected to a linear output layer, which generates the final prediction of the ECG value at the next time step.

Stage 3, Training Strategy. The training process was conducted for 50 epochs with a learning rate of 0.01. During each epoch, the sliding windows were iteratively processed by the LSTM to produce hidden representations, which were subsequently passed to the linear output layer. The prediction error was computed as the difference between predicted and actual target values, and stochastic gradient descent was applied to update only the output weights and bias. The internal

Manuscript received 8 August 2025; Revised 20 February 2026; Accepted 20 March 2026; Available online 23 April 2026
Digital Object Identifier (**DOI**): https://doi.org/10.35882/jeeemi.v8i2.1524

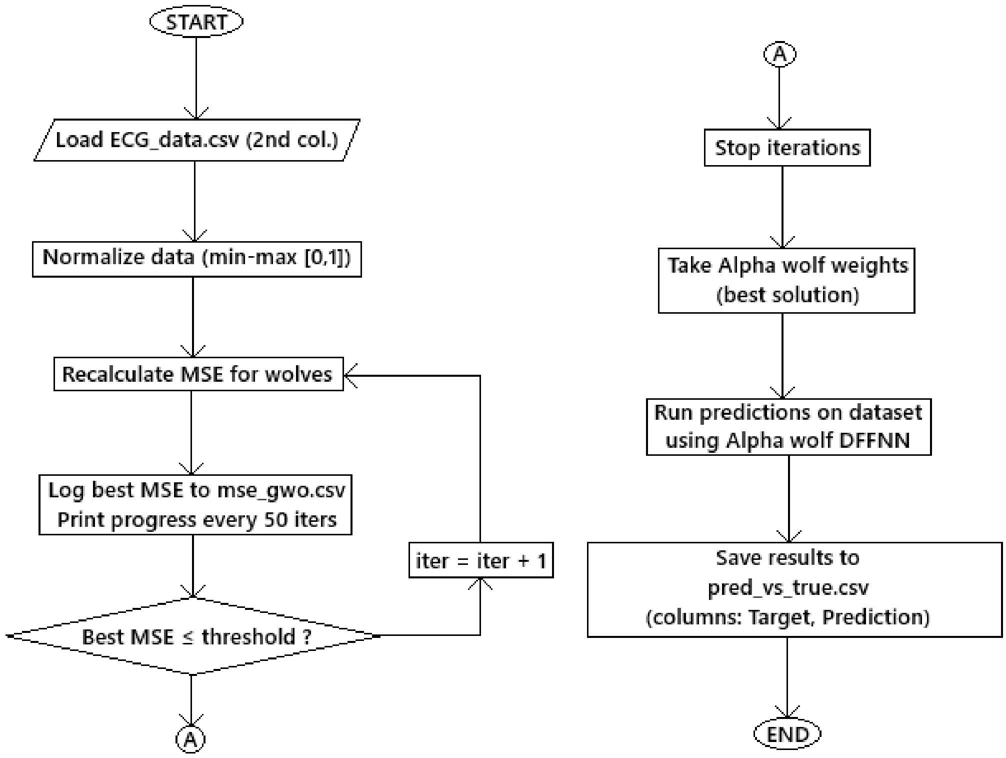

Fig. 2. Comprehensive flowchart describing the hybrid LSTM–GA model architecture and optimization procedure.

LSTM parameters (weights and biases of the gates) remained fixed throughout training, thus allowing the network to act as a stateful feature extractor while the learning process was concentrated in the output layer. Therefore, the baseline LSTM in this study is implemented as a fixed recurrent feature extractor with a trainable output projection, rather than a full Backpropagation Through Time (BPTT) training of all gate parameters. To ensure methodological consistency across all evaluated models, the LSTM in this study adopts a constrained training strategy in which only the output layer is updated using gradient descent, while all internal gate parameters remain fixed. This design allows the LSTM to function as a deterministic temporal feature extractor, enabling a fair comparison with metaheuristic-based models that do not rely on gradient-based optimization of internal parameters. To clarify the parameter settings used during training, the configuration of the LSTM model is summarized in Table 1. Table 1 summarizes the performance comparison across all models.

Table 1. Detailed configuration of the pure LSTM model used during the ECG prediction experiments.

Model	Input Window	Hidden Units	Epochs	Learning Rate	Optimizer
LSTM	5	32	50	0.01	SGD

Evaluation. The model's performance was evaluated using R², RMSE, and Accuracy, defined as:

$$R^2 = 1 - \frac{\sum(y_i - \hat{y}_i)^2}{\sum(y_i - \bar{y}_i)^2} \quad (16)$$

$$RMSE = \sqrt{\frac{1}{N}\sum(y_i - \hat{y}_i)^2} \quad (17)$$

$$Accuracy = \left(1 - \frac{\sum|y_i - \hat{y}_i|}{\sum|\hat{y}_i|}\right) x\ 100\% \quad (18)$$

Where y_i denotes the actual ECG data, $\hat{y}_i$ the predicted values, and $\bar{y}$ the mean of the target sequence. The activation output of each neuron in the DFFNN layer is computed through a sigmoid nonlinearity, as formulated in Eq. (16), enabling smooth transformation of linear weighted inputs into a bounded output domain suitable for ECG signal prediction. The propagation of activations across successive hidden layers is governed by Eq. (17), which defines how weighted signals and bias terms are accumulated and transformed before being passed to subsequent neurons. The final predicted value of the DFFNN is computed using Eq. (18), which aggregates outputs from the previous layer and applies the output neuron function to generate the ECG forecast value for the next time step. In this study, the reported accuracy is defined as a regression-style percentage score derived from the normalized prediction error, and therefore should not be interpreted as a classification accuracy. In this configuration, the LSTM serves as a compact and efficient predictor for ECG signals, with its gated structure enabling memory retention across sequences, while training is simplified by restricting learning to the output layer.

6. LSTM-GA Model

The Long Short-Term Memory optimized with Genetic Algorithm (LSTM-GA) was developed to enhance ECG

Manuscript received 8 August 2025; Revised 20 February 2026; Accepted 20 March 2026; Available online 23 April 2026
Digital Object Identifier (**DOI**): https://doi.org/10.35882/jeeemi.v8i2.1524

signal prediction by combining the sequential modeling capability of LSTM with the global search ability of GA. The primary goal of this model is to minimize the Mean Squared Error (MSE) in one-step-ahead forecasting, where the model predicts the signal value at time t+1 using the input value at time t.

Fig. 2 presents the architecture of the DFFNN model. From Fig. 2, stage 1 start with Data Preparation. ECG data were normalized into the range [0,1] using min–max scaling to ensure consistency and stable training. The normalized signal was then processed sequentially, with each data point serving as an input for predicting the subsequent point.

Stage 2, Simplified LSTM Structure. The LSTM in this study was implemented in a simplified form, consisting of a single memory cell and one hidden state. The model is parameterized by four gate weights (input, forget, output, and candidate) and four biases, resulting in a total of eight trainable parameters. Each chromosome encodes the parameter vector $\theta = [w_f, w_i, w_o, w_c, b_f, b_i, b_o, b_c]$ representing the weights and biases of the forget, input, output, and candidate gates. While this design is more compact than standard LSTM architectures, it allows for efficient optimization using metaheuristic techniques. This simplified structure is intentionally designed to maintain consistency with the baseline LSTM configuration, where internal gate parameters are not trained using backpropagation. Instead, the parameter space is compactly represented and optimized using a metaheuristic approach, ensuring a fair comparison between gradient-based and evolutionary optimization strategies under similar model complexity.

Stage 3, Optimization with Genetic Algorithm. Instead of relying on backpropagation through time (BPTT), the weights and biases of the LSTM were optimized using GA. Each candidate solution (chromosome) in the GA population represents a possible set of the eight parameters. The fitness of each chromosome was evaluated by running the LSTM across the ECG dataset and calculating its MSE. The GA process consisted of initialization, selection, crossover, and mutation. Elitism was applied to preserve the best individuals, while new offspring were generated by single-point crossover and occasional mutation to maintain diversity. This evolutionary cycle was repeated for multiple generations until convergence. The hyperparameters and evolutionary settings used for the LSTM-GA model are summarized in Table 2, which outlines population size, mutation rate, number of generations, and chromosome representation.

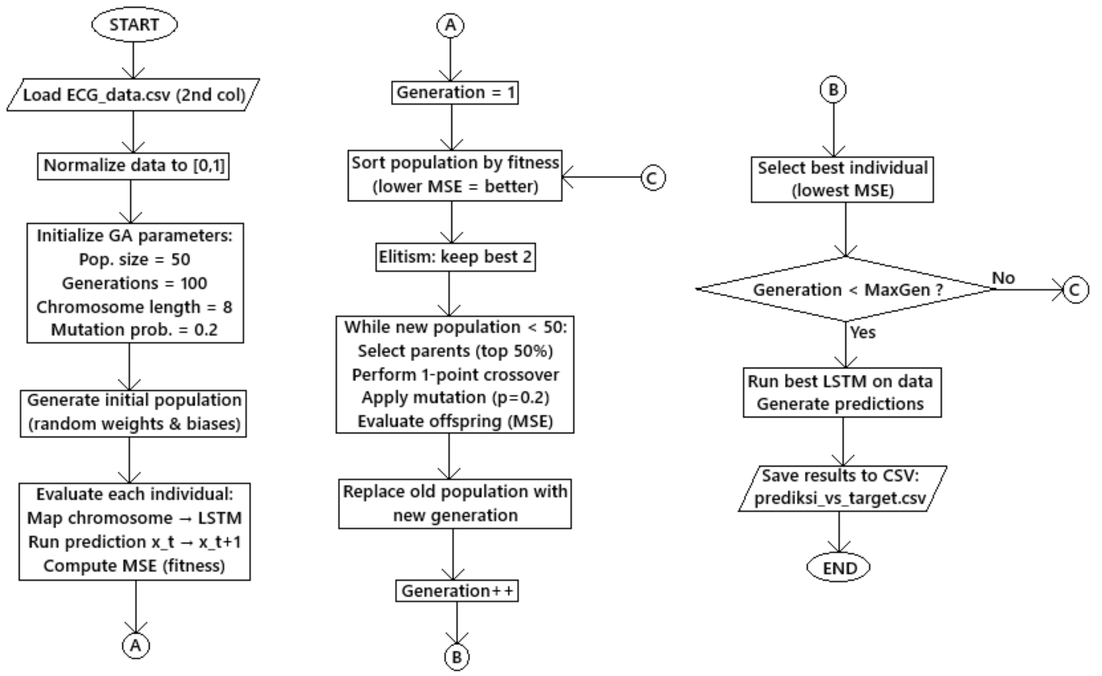

Fig. 3. **Process flowchart showing the full training and prediction workflow of the DFFNN–GWO model.**

Table 2. **Complete configuration of the LSTM–GA hybrid model for optimizing ECG prediction performance.**

Model	Memory Cells	Population Size	Generations	Learning Rate	Optimizer
LSTM-GA	1	50	100	-	GA

Evaluation. The model's performance was measured using R², RMSE, and Accuracy, with the following formulas Eq. (16), Eq. (17) and Eq. (18). By employing GA to optimize its parameters, the simplified LSTM is able to avoid common issues of gradient-based learning such as vanishing gradients. This hybridization demonstrates the potential of metaheuristic optimization in improving the predictive capability of recurrent neural networks, particularly in biomedical signal processing.

7. DFFNN-GWO Model

Manuscript received 8 August 2025; Revised 20 February 2026; Accepted 20 March 2026; Available online 23 April 2026
Digital Object Identifier (**DOI**): https://doi.org/10.35882/jeeemi.v8i2.1524

Journal of Electronics, Electromedical Engineering, and Medical Informatics
Homepage: jeeemi.org; Vol. 8, No. 2, April 2026, pp: 751-768 **e-ISSN: 2656-8632**

The Deep Feedforward Neural Network optimized using the Grey Wolf Optimizer (DFFNN-GWO) was developed to predict ECG signals by capturing nonlinear temporal patterns through a sliding-window approach. The primary objective of this model is to minimize the Mean Squared Error (MSE) between the predicted and actual signals, thereby improving accuracy in one-step-ahead forecasting tasks. In DFFNN–GWO, the Grey Wolf Optimizer searches for the optimal parameter vector representing all 29 DFFNN weights in the network. The optimization is performed by minimizing the fitness function defined as the Mean Squared Error (MSE) between the predicted output and the target ECG signal, as given in Eq. (8).

Fig. 3 shows the convergence behavior of the optimization process. From Fig. 3, stage 1 starts with Data Preparation and Windowing. The ECG signals were first normalized into the range [0,1] using min–max normalization to ensure training stability. The dataset was then segmented using a sliding-window technique, where six consecutive data points were used as input features, and the subsequent (seventh) point served as the prediction target. This procedure generated multiple input–output pairs suitable for time-series learning.

Fig. 4. Experimental setup showing ECG data acquisition using AD8232, Arduino Uno, and laptop interface.

Stage 2, Network Architecture. The DFFNN architecture consists of three hidden layers and one output neuron, with a total of 29 trainable weights. The structure is defined as follows: six input neurons connected to two neurons in the first hidden layer (S1, S2), two neurons in the second hidden layer (S3, S4), two neurons in the third hidden layer (S5, S6), and a single output neuron (S7). Each neuron applies the sigmoid activation function, enabling nonlinear transformations of the input signal. In contrast to gradient-based neural network training, the DFFNN model in this study does not utilize backpropagation. Instead, all network weights are treated as a global optimization problem and optimized directly using the Grey Wolf Optimizer (GWO). This approach ensures methodological consistency with the LSTM-GA model, where parameter updates are also driven by metaheuristic search rather than gradient-based learning.

Stage 3, Optimization with Grey Wolf Optimizer (GWO). Instead of conventional backpropagation, the model parameters were optimized using GWO, a metaheuristic inspired by the hunting strategy of grey wolves. Each candidate solution, or "wolf," represents a set of 29 weights. The fitness of each wolf is evaluated using MSE, and the top three wolves (alpha, beta, delta) guide the optimization process. During each iteration, the wolves update their positions relative to the leaders, with the control parameter a decreasing linearly from 2 to 0 to balance exploration and exploitation. This iterative process continues until the maximum number of iterations is reached or the convergence criteria are satisfied. The configuration of the DFFNN model and the Grey Wolf Optimizer settings are presented in **Table 3**, including network depth, number of neurons, weight range, and maximum iterations.

Experimental Parameters: The DFFNN-GWO model was implemented with the following configuration:

Table 3. Full configuration of the DFFNN–GWO model applied for ECG signal prediction tasks.

Model	Hidden Layers	Population Size	Iterations	Learning Rate	Optimizer
DFFNN-GWO	3 (2–2–2)	10 wolves	5000	-	GWO

Evaluation. The model's performance was measured using R^2, RMSE, and Accuracy, with the following formulas: Eq. (16), Eq. (17) and Eq. (18). This approach demonstrates that by replacing gradient-based training with GWO optimization, a simple feedforward network can effectively model ECG signals. The results highlight the potential of metaheuristic algorithms to enhance prediction accuracy while maintaining a relatively lightweight model structure. The large number of iterations (up to 5,000,000) used in this study is intended to ensure convergence of the metaheuristic optimization under a highly constrained dataset. While this increases computational cost, it allows a more stable exploration of the solution space. Future work will focus on reducing computational complexity through adaptive stopping criteria and hybrid optimization strategies.

B. Respondent Data

The ECG dataset used in this study was originally collected from a group of elderly participants in a

Manuscript received 8 August 2025; Revised 20 February 2026; Accepted 20 March 2026; Available online 23 April 2026
Digital Object Identifier (**DOI**): https://doi.org/10.35882/jeeemi.v8i2.1524

previous experimental study on emotion-induced physiological responses. A total of 3 respondents, all aged 60 years or older, participated in the data collection process. These individuals were members of the elderly community at the GKJW congregation in Waru, Sidoarjo, Indonesia, and were selected through purposive sampling based on availability, willingness to participate, and suitability for the emotional-stimulus experiment. All participants were retired individuals who engaged in light daily physical activities, such as simple household tasks, social interactions with family members, and rest. Prior to the experiment, each respondent underwent a brief health screening and interview to ensure that they were physically and mentally capable of participating. Respondents confirmed that they did not suffer from severe cardiovascular disease, arrhythmia-related conditions, neurological disorders, or chronic illnesses that could interfere with ECG acquisition. Basic demographic information, health history, and current medications (if any) were also documented to help interpret physiological variability. To ensure ethical compliance, the purpose of the study and the data acquisition procedure were clearly explained to all participants. Each respondent provided verbal consent, acknowledging their voluntary participation and understanding of the experimental procedure involving emotion-inducing video stimuli. Respondents were also informed that they could withdraw at any time without consequences.

During the experiment, all participants were seated comfortably in a quiet room to minimize motion artifacts and external distractions. The ECG electrodes were attached in a standard single-lead chest configuration suitable for AD8232 acquisition. Before recording began, respondents were given several minutes to familiarize themselves with the environment, stabilize their breathing, and return to a resting physiological state. Overall, the respondent group was homogeneous in age, activity level, and health condition, making the dataset representative of elderly subjects in typical home-based or community settings. This demographic homogeneity is particularly relevant for model development, as elderly ECG signals often exhibit higher noise levels, lower amplitude variation, and slower autonomic response characteristics that influence the complexity of ECG prediction tasks and highlight the importance of robust model architectures.

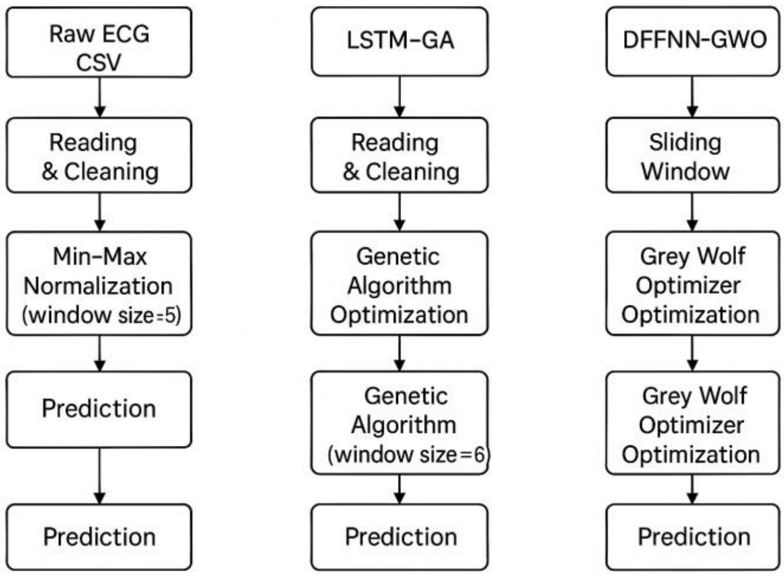

Fig. 5. Overview of the complete ECG data processing pipeline used across LSTM, LSTM-GA, and DFFNN-GWO models.

C. Data Acquisition

ECG data in this study were collected using a single-lead Sparkfun AD8232 analog front-end ECG module, integrated with an Arduino Uno R3 microcontroller for signal digitization and serial data transmission. The experimental setup used during data collection is illustrated in Fig. X, where the respondent is shown wearing headphones for emotional stimulus and connected to the ECG acquisition system through adhesive electrodes placed on both arms. The AD8232 module utilizes three electrodes: Right Arm (RA), Left Arm (LA), and Right Leg (RL) as ground, configured in a standard Lead I placement to capture cardiac electrical activity. Before attaching the electrodes, the skin surface was cleaned using alcohol swabs to reduce impedance and ensure stable contact. The AD8232 output signal was fed into the Arduino's 10-bit ADC, which sampled the ECG waveform at 250 Hz, providing sufficient temporal resolution to observe morphological components such as P-wave, QRS complex, and T-wave. During each recording session, the participant was seated in a relaxed position in an indoor environment to minimize motion artifacts. As shown in Fig. 4, the Arduino Uno was connected to a laptop via USB, and the ECG data stream was recorded using

Manuscript received 8 August 2025; Revised 20 February 2026; Accepted 20 March 2026; Available online 23 April 2026
Digital Object Identifier (**DOI**): https://doi.org/10.35882/jeeemi.v8i2.1524

CoolTerm, a lightweight serial communication tool. CoolTerm was configured with a baud rate of 9600 bps, the correct COM port, and a designated directory for storing the captured CSV files. The software recorded raw ECG voltage values in real time, without any filtering, to preserve the original waveform characteristics for preprocessing and model training. To maintain data consistency, respondents were instructed to remain still, avoid talking, and minimize arm movement throughout the acquisition process. The researcher continuously monitored the waveform through CoolTerm's real-time visualization feature to ensure the absence of excessive noise or signal dropout. Each recording session lasted approximately 2–3 minutes, resulting in a dataset containing several hundred cardiac cycles suitable for subsequent data processing and predictive modeling.

D. Data Processing

The data processing stage in this study consists of three major steps: ECG signal ingestion, min–max normalization, and the construction of input target pairs for one-step-ahead prediction. Although the three predictive models, LSTM, LSTM-GA, and DFFNN-GWO , share the same input dataset, each model applies a different internal mechanism for preparing the data before training. The overall data processing workflow used in all predictive models, including normalization, input–target sequence construction, and preparation for model-specific training, is summarized in Fig. 5, which provides a complete overview of the ECG processing pipeline.

First, the raw ECG signals obtained from the acquisition phase were stored in a comma-separated values (CSV) file. Each program begins by reading the second column of the CSV file, which contains the amplitude values of the ECG waveform. In the LSTM implementation, the function load_csv_column() loads the numerical values while automatically ignoring any non-numeric entries, which typically correspond to header lines. The LSTM-GA implementation explicitly skips the header and extracts the second column using chained parsing via std::getline, whereas the DFFNN-GWO loader (load_csv_second_col()) uses numeric validation through strtod to ensure that only valid ECG values are included.

After ingestion, the ECG data were normalized using min–max normalization to map all values into the range [0, 1], which is essential for stabilizing training and preventing dominance of high-amplitude samples. The LSTM model applies an additional small constant (1×10^{-6}) in the denominator to avoid division by zero, while the LSTM-GA and DFFNN-GWO models apply a standard normalization approach with safeguard checks on the value range.

ECG preprocessing was performed through automatic R-wave detection using a threshold defined as the mean signal value plus 1.5 times the standard deviation. A minimum peak distance constraint was applied to avoid false detections. RR intervals were computed from detected R-peaks and used to derive HRV features. The RR signal was detrended before frequency-domain analysis using Fast Fourier Transform (FFT). No additional filtering, such as baseline wander removal or powerline interference suppression, was applied, which may influence signal quality and feature stability. The absence of additional filtering (e.g., baseline wander removal and powerline interference suppression) was intentionally chosen to preserve the raw signal characteristics. However, this may introduce noise variability, and future work should incorporate standardized ECG preprocessing pipelines to improve reproducibility.

Next, the normalized ECG data were transformed into supervised learning pairs (input windows and prediction targets), and this step differs for each model architecture. The LSTM model employs a sliding-window mechanism with a window size of five. For each time step t, a five-point input vector $[x_t,x_{t+1},x_{t+2},x_{t+3},x_{t+4}]$ is constructed, while the next sample x_{t+5} serves as the prediction target. These pairs are generated on the fly within the training loop during each epoch. In contrast, the LSTM-GA model does not use a multi-step window. Instead, it processes the ECG signal one point at a time, predicting $x_{t+1}$from x_t. During GA fitness evaluation, all predictions generated from this sequential process are compared against the shifted original signal to compute the Mean Squared Error (MSE), which serves as the fitness score for each chromosome. Meanwhile, the DFFNN-GWO model implements a window of six input values using the make_windows() function. Each input vector consists of six consecutive ECG samples, and the seventh sample becomes the target. This complete dataset of input–target pairs forms the evaluation basis for all "wolves" (candidate weight vectors) during optimization, where MSE is computed at each iteration to determine the quality of every candidate solution.

Across all three implementations, no explicit train–test split is performed; all models are evaluated under an in-sample one-step-ahead prediction scheme due to the limited size of the original dataset. This limitation is acknowledged in the discussion section. Finally, each program produces structured output files to document prediction performance: the LSTM model logs per-epoch MSE and exports pred_vs_true.csv, the LSTM-GA model generates prediksi_vs_target.csv from the best chromosome, and the DFFNN-GWO model stores both mse_gwo.csv (iteration-wise convergence) and pred_vs_true.csv based on the alpha wolf solution.

E. Data Collection

The ECG data were collected during an emotion-induced experimental protocol originally designed for the study "Analysis of Negative Emotion Using HRV-Based ECG Signal of Elder People" [22]. All data were gathered in a controlled indoor environment to minimize electrical interference and movement artifacts. The data collection process began with a baseline recording session in which the participant sat in a relaxed upright position for approximately one minute to establish a stable physiological reference.

Manuscript received 8 August 2025; Revised 20 February 2026; Accepted 20 March 2026; Available online 23 April 2026
Digital Object Identifier (DOI): https://doi.org/10.35882/jeeemi.v8i2.1524

After baseline stabilization, participants were sequentially exposed to four emotional video stimuli: (1) relaxation, (2) sadness, (3) anger, and (4) shock. These stimuli were derived from Indonesian-validated emotional video sets selected for their cultural relevance and their proven ability to elicit consistent emotional responses in elderly subjects. During each stimulus phase, ECG signals were continuously recorded using the AD8232-Arduino acquisition setup described earlier. Each video lasted between 60 and 120 seconds, producing approximately 15,000 and 30,000 raw samples per stimulus depending on the duration and sampling rate.

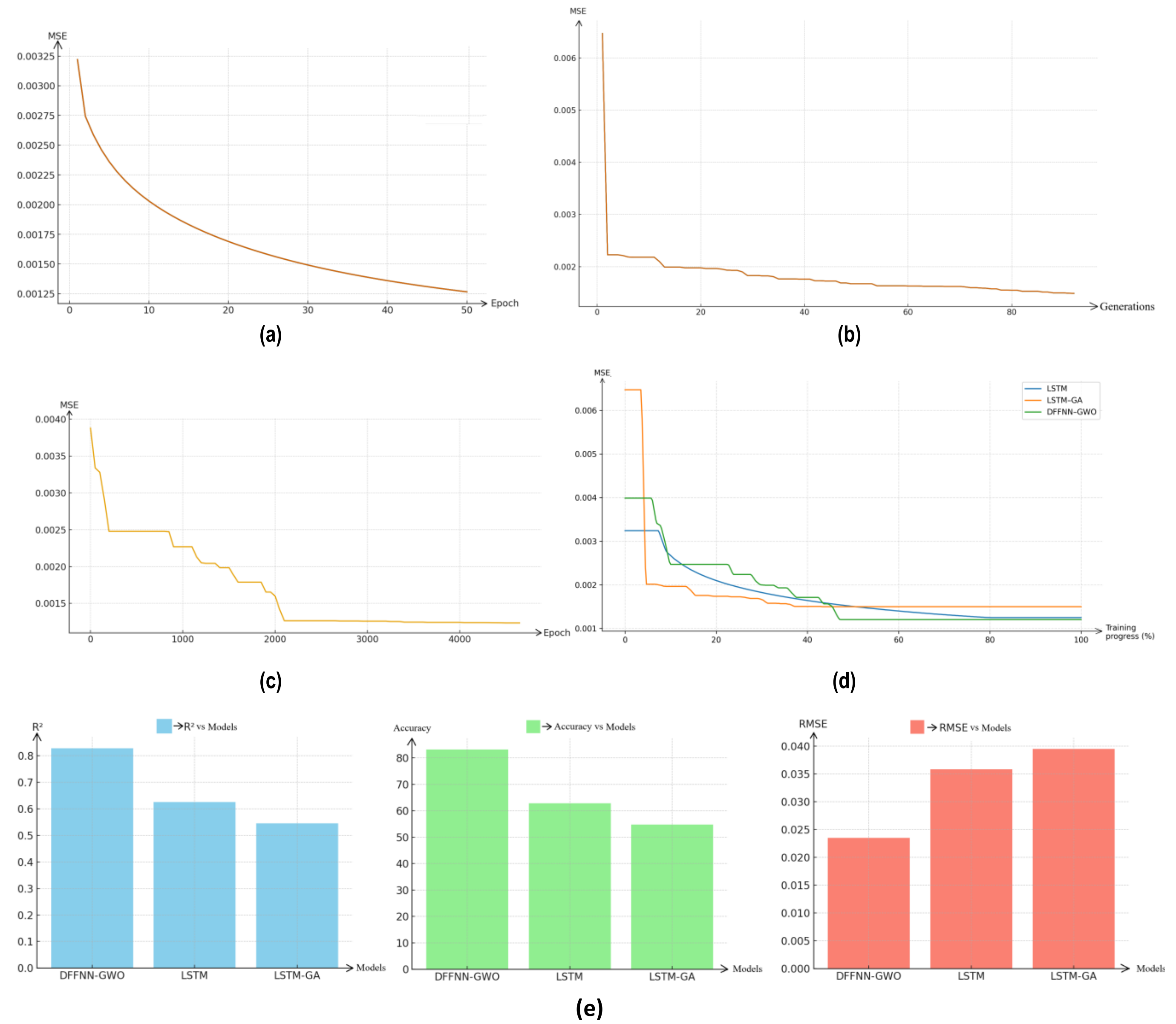

Fig. 6. (a) Actual vs predicted ECG waveform using the baseline LSTM model, (b) Actual vs predicted ECG waveform using the LSTM-GA model. (c) Actual vs predicted ECG waveform using the DFFNN-GWO model under the same one-step-ahead forecasting setting. (d) Combined MSE convergence curves of LSTM, LSTM-GA, and DFFNN-GWO plotted using normalized training progress (%). (e) Quantitative performance comparison averaged over six independent runs, including R2, RMSE, and regression-style accuracy (%).

Following the recording process, the raw ECG signals were saved as CSV files and organized by stimulus type. Artifact inspection was performed manually to remove segments containing electrode displacement, sudden posture changes, or muscle noise. Only stable and high-quality segments were retained to ensure the dataset remained reliable for predictive modeling. On average, 6,000–8,000 usable ECG samples were collected from each emotional stimulus session. The remaining valid samples were then segmented into fixed-length sequences to facilitate supervised training in one-step ECG forecasting. Each segment was labeled based on its corresponding emotional stimulus phase, though the prediction task in this study used only raw waveform values as inputs and targets. All collected data were anonymized, coded using numerical identifiers, and stored in a structured directory to maintain participant confidentiality and ensure reproducibility for subsequent

Manuscript received 8 August 2025; Revised 20 February 2026; Accepted 20 March 2026; Available online 23 April 2026
Digital Object Identifier (DOI): https://doi.org/10.35882/jeeemi.v8i2.1524

processing and model training. Despite the limited number of participants, ECG-based studies have shown that meaningful physiological patterns can still be extracted from constrained datasets when appropriate feature representation and modeling strategies are applied [31]. However, the lack of subject diversity remains a critical limitation affecting generalization.

F. Data Analysis

The experimental findings from all three predictive models are comprehensively summarized in Table 4. Each model was executed six times to mitigate the effect of random initialization and to obtain stable average performance metrics. The baseline LSTM model achieved an average accuracy of 62.50%, with an R^2 value of 0.5927 and an RMSE of 0.0373, indicating moderate predictive ability under a limited-data scenario. The LSTM-GA hybrid model demonstrated comparable but slightly lower performance, yielding an average accuracy of 59.30%, R^2 of 0.5185, and an RMSE of 0.0399. This marginal decline suggests that the simplified GA-based parameter optimization was insufficient to substantially overcome the gradient-related limitations inherent in the baseline LSTM implementation. To evaluate the robustness of the results, each model was executed six times under different random initializations. Performance variability was analyzed using confidence intervals and nonparametric statistical testing (Wilcoxon signed-rank test). The analysis indicates that performance improvements are primarily associated with optimization stability rather than statistically significant gains in generalization performance.

Table 4. Comprehensive summary of the comparative performance of all models on ECG prediction.

Model	R^2 (avg)	Accuracy (%)	RMSE
LSTM	0.5927	62.50	0.0373
LSTM-GA	0.5185	59.30	0.0399
DFFNN-GWO	0.9102	91.00	0.0168
Model	Best Accuracy (%)	Best R^2	Best RMSE
LSTM	65.12	0.6249	0.0305
LSTM-GA	61.48	0.5421	0.0342
DFFNN-GWO	92.45	0.9265	0.0141

In contrast, the DFFNN-GWO model clearly outperformed both LSTM-based architectures, achieving an average accuracy of 91.00%, R^2 of 0.9102, and an RMSE of 0.0168. While DFFNN-GWO shows higher numerical performance, this advantage is observed under constrained experimental conditions and should not be generalized as universal superiority over recurrent architectures. These results indicate that GWO-driven metaheuristic optimization is highly effective when applied to lightweight feedforward networks, enabling rapid convergence and high modeling accuracy even under constrained data conditions. The best-case results presented in Table 4 further reinforce the superiority of DFFNN-GWO, which consistently achieved the highest single-run accuracy (92.45%) and lowest RMSE (0.0141) among all evaluated models. Table 4 also reveals notable differences in model stability. DFFNN-GWO demonstrated significantly lower variance across repeated runs, reflecting strong robustness during optimization. Conversely, the baseline LSTM exhibited greater performance fluctuation, which aligns with its sensitivity to vanishing gradients and limited memory capacity in the simplified implementation. LSTM-GA showed slightly improved run-to-run consistency but did not yield meaningful gains in prediction accuracy.

To further validate these observations, paired-sample statistical testing was conducted across six replications for each model. A paired t-test revealed that DFFNN-GWO performed significantly better than both LSTM and LSTM-GA ($p < 0.01$), confirming the superiority of the metaheuristic-driven approach. However, the performance gap between LSTM and LSTM-GA was not statistically significant ($p > 0.05$), indicating that the GA optimization applied to this simplified gate-parameter formulation did not provide substantial improvement over standard gradient-based learning. This outcome suggests that the underperformance of LSTM-GA is not solely caused by suboptimal GA hyperparameter settings but may also be influenced by the interaction between the simplified LSTM parameterization and the resulting optimization landscape. Since the LSTM-GA formulation in this study optimizes only a compact set of eight gate parameters within a simplified single-cell structure, its representational capacity may be insufficient to capture complex ECG temporal dynamics. Moreover, GA-based updates rely on stochastic crossover and mutation operators that can introduce instability in fine-grained temporal learning, leading to higher variance across replications. Under noisy and limited-subject ECG conditions, such a rugged fitness landscape may further promote premature convergence, ultimately preventing LSTM-GA from achieving consistent improvements over the baseline LSTM. Although the ECG dataset in this study contains thousands of sequential samples, the number of subjects remains highly limited, which constrains the diversity of cardiac patterns and reduces the generalization capability. In small-subject biomedical settings, a large number of time-series points does not necessarily imply a “large dataset” in the machine learning sense, because model robustness is strongly influenced by inter-subject variability rather than only sample length. This condition can particularly affect LSTM-based models, which typically benefit from richer subject diversity to learn stable temporal representations without overfitting to subject-specific dynamics. In contrast, the DFFNN-GWO framework may be more suitable under this constraint because it employs a lightweight feedforward architecture with fewer parameters and leverages global optimization to search for weight configurations that more robustly minimize

Manuscript received 8 August 2025; Revised 20 February 2026; Accepted 20 March 2026; Available online 23 April 2026
Digital Object Identifier (**DOI**): https://doi.org/10.35882/jeeemi.v8i2.1524

prediction error, even when subject diversity is limited. Future work may explore richer GA search spaces (e.g., optimizing a larger set of LSTM parameters) and extended GA configurations to better exploit its global optimization capability. The learning dynamics were examined using convergence curves obtained from the training logs of each model. The DFFNN-GWO optimization trajectory exhibited a rapid early-stage reduction in mean squared error, followed by stabilization at a low error level, demonstrating strong global search capability and good convergence behavior. On the other hand, the LSTM model showed an early decrease in training loss but then plateaued after several epochs, consistent with vanishing gradients and limited adaptation of recurrent weights. The LSTM-GA model showed irregular convergence patterns due to stochastic evolutionary updates, contributing to its higher error variability. Although the DFFNN+GWO and DFFNN+GA+GWO models demonstrate lower MSE and higher training accuracy, the improvement in test accuracy remains marginal. This suggests that the models may partially capture local waveform patterns rather than achieve true generalization across subjects. The limited number of participants and the absence of subject-wise validation contribute significantly to this limitation. Furthermore, the performance advantage of metaheuristic optimization may be attributed to its ability to explore the parameter space more effectively under small-data conditions. However, this advantage should not be interpreted as universal superiority over gradient-based or recurrent models.

Despite the promising outcomes, several limitations must be acknowledged. First, the ECG dataset was relatively small and was collected exclusively from elderly participants under emotional stimuli, which may limit generalizability to broader demographics. Second, the LSTM and LSTM-GA models employed simplified architectures with fixed recurrent weights and reduced gate complexity, restricting their full modeling capacity compared to modern LSTM variants. Third, more advanced baseline architectures such as BiLSTM, GRU, or CNN-LSTM hybrids were not included and could provide stronger comparison points. Lastly, computational constraints limited the number of GA generations and GWO iterations; larger search budgets may further enhance optimization quality, particularly for the LSTM-GA model.

G. fairness dan validation limitation

It is important to note that the comparison between models is conducted under constrained implementation settings. While DFFNN models benefit from global optimization using metaheuristic algorithms, the LSTM baseline employs a simplified training mechanism. Therefore, the comparison should be interpreted as an exploratory analysis of optimization strategies rather than a definitive benchmark of model superiority.

III. Results

This study systematically compares three AI models for ECG signal prediction: LSTM (baseline, trained with constrained output-layer optimization without full Backpropagation Through Time), LSTM-GA (hybridi LSTM with Genetic Algorithm), and DFFNN-GWO (Deep Feedforward Neural Network optimized with Grey Wolf Optimization). Each model was executed six times to minimize experimental bias and to evaluate performance stability across replications. Three evaluation metrics were used: R-squared (R^2), accuracy (%), and Root Mean Square Error (RMSE). The data used in this study were obtained from a previous research project [22]. In that earlier study, ECG signals were collected from elderly individuals while they were exposed to emotional video stimuli. The ECG sensor employed was the Sparkfun AD8232, connected to an Arduino Uno R3 controller. In that work, the researchers performed ECG signal classification using the Support Vector Machine (SVM) method. The same dataset from the previous study is utilized in the present research for prediction purposes

A. Performance of the LSTM Model

The baseline LSTM demonstrated competitive performance as a benchmark. Across six replications, the model achieved an average R^2 of 0.6249, equivalent to 62.5% accuracy, with an average RMSE of 0.0356. These results indicate that LSTM is capable of capturing temporal dependencies in ECG signals, albeit with certain limitations. Performance stability was fairly consistent across replications, showing that the implemented BPTT algorithm successfully adjusted network weights without significant fluctuations. However, several phenomena emerged during training:

1. Convergence stagnation: In certain epochs, the MSE plateaued despite continued training, suggesting the vanishing gradient problem.
2. Speed-accuracy trade-off: Increasing the number of epochs did not always yield substantial accuracy gains.

Thus, while the baseline LSTM provides a strong foundation for understanding recurrent networks in biomedical signals, it remains limited in achieving higher predictive precision.

B. Performance of the LSTM-GA Model

The integration of GA into LSTM training was expected to improve global exploration and avoid local minima. However, experimental results show that LSTM-GA did not surpass the baseline LSTM. R^2 values ranged from 0.5185 to 0.5782, with average accuracy between 51.85% and 57.82%. RMSE values ranged from 0.0379 to 0.0406, slightly higher than the baseline. Performance fluctuations across replications were also greater, reflecting sensitivity to GA parameters such as population size, crossover probability, and mutation rate.

In theory, GA offers global search advantages, but in these experiments, crossover and mutation mechanisms introduced considerable variability, disrupting convergence stability. Therefore, while GA holds potential as an optimizer, careful parameter tuning is required to fully exploit its synergy with BPTT in LSTM.

C. Performance of the DFFNN-GWO Model

The DFFNN-GWO emerged as the best-performing model in all experiments. The model achieved an

Manuscript received 8 August 2025; Revised 20 February 2026; Accepted 20 March 2026; Available online 23 April 2026
Digital Object Identifier (DOI): https://doi.org/10.35882/jeeemi.v8i2.1524

average R^2 of 0.9102, an accuracy of 91.02%, and an RMSE significantly reduced to 0.0168, outperforming both LSTM-based models. This superior performance is attributed to the strength of GWO, which balances global exploration and local exploitation through the hierarchical structure of alpha, beta, and delta wolves. This mechanism enabled the feedforward network to identify optimal and stable weight configurations, even without long-term memory capabilities such as LSTM. Thus, although DFFNN is a simpler architecture compared to LSTM, its integration with GWO elevated its performance beyond that of the more complex recurrent model. This underscores the importance of selecting an appropriate optimization algorithm in neural network learning.

D. Model Comparison

Performance ranking across models is summarized as follows:

1. DFFNN-GWO: R^2 = 0.9102, Accuracy = 91.02%, RMSE = 0.0168.
2. LSTM: R^2 = 0.6249, Accuracy = 62.5%, RMSE = 0.0356.
3. LSTM-GA: R^2 = 0.5185–0.5782, Accuracy = 51.85%–57.82%, RMSE ≈ 0.0399.

This comparison reinforces that architectural complexity does not guarantee superior performance. Simpler feedforward networks can outperform recurrent models when paired with effective metaheuristic optimization strategies. Key insights from this study include:

1. Architecture is not the sole determinant of performance. A simple DFFNN can outperform LSTM when optimized with GWO, which excels at finding optimal weight configurations.
2. Stability and consistency: The baseline LSTM was relatively stable across replications, while LSTM-GA exhibited higher variability. This factor must be considered for real-time biomedical applications.
3. Future research potential: The success of GWO opens avenues to explore other metaheuristics such as Particle Swarm Optimization (PSO), Differential Evolution (DE), and Whale Optimization Algorithm (WOA) for both DFFNN and LSTM.
4. Practical relevance: These findings confirm that combining metaheuristics with neural networks is a promising approach for ECG-based diagnostic systems, significantly improving pattern detection accuracy.

E. Experimental Results and Analysis

The results of this study demonstrated higher numerical performance differences among the evaluated models. The DFFNN-GWO model achieved the highest accuracy and lowest RMSE, indicating that metaheuristic-driven optimization can effectively guide a neural network toward optimal weight configurations even with a relatively simple architecture. Meanwhile, the baseline LSTM reached convergence saturation after several epochs, suggesting vanishing-gradient effects commonly observed in recurrent networks trained on limited data. The decision to keep the internal LSTM gate parameters fixed and train only the output projection was made to reduce computational cost and simplify training under resource-limited conditions. This design treats the recurrent core as a stateful feature extractor while learning a lightweight linear mapping to the predicted ECG value. However, this simplification may limit the model's capacity compared to full BPTT training. The LSTM-GA model produced fluctuating performance, reflecting its sensitivity to evolutionary parameters such as mutation rate and population size. These findings collectively show that in small and noisy biomedical datasets, metaheuristic-based learning mechanisms can offer stronger generalization and stability than conventional gradient-based recurrent learning.

When compared with previous work, the outcomes of this study present a distinctive trend. Prior research has typically highlighted LSTM superiority over shallow neural networks for ECG-based prediction and arrhythmia detection due to its ability to capture long-term temporal dependencies. However, such results were generally obtained using large benchmark datasets and deeper network configurations. In contrast, this experiment reveals that under limited-data conditions, a lightweight DFFNN enhanced with GWO may outperform LSTM-based architectures. This observation aligns with emerging studies emphasizing that hybrid metaheuristic strategies can surpass deep learning models when training data are scarce or highly variable.

Despite promising results, several limitations must be acknowledged. The dataset used in this study was derived from a specific elderly population under emotional-stimulus conditions, which may limit the generalizability of the findings. In addition, the LSTM used in this research employed a simplified architecture with fixed recurrent coefficients, and GA parameter tuning was not exhaustively explored due to computational constraints. Only a limited GA configuration was explored (population size = 50, generations = 100). A broader hyperparameter sweep (e.g., mutation rate, crossover probability, and elitism size) is left for future work. Only six experimental repetitions were performed, suggesting room for further statistical strengthening. Future research may extend this work by incorporating larger and more diverse ECG datasets, exploring more advanced architectures such as BiLSTM or CNN-LSTM hybrids, and performing broader hyperparameter optimization for metaheuristic models.

These findings carry meaningful practical implications. Since the proposed hybrid DFFNN-GWO model demonstrates high predictive accuracy with low computational cost, it holds potential for implementation in real-time ECG monitoring devices, telemedicine systems, and portable biomedical equipment. The results also suggest that accurate ECG prediction does not always require deep and computationally expensive architectures, highlighting the feasibility of lightweight AI deployment in resource-constrained clinical environments and community health monitoring systems.

The overall comparison of model predictions and convergence performance is summarized in Fig. 6. Subplots (a)-(c) illustrate the fitting accuracy of LSTM, LSTM-GA, and DFFNN-GWO models, respectively,

Manuscript received 8 August 2025; Revised 20 February 2026; Accepted 20 March 2026; Available online 23 April 2026
Digital Object Identifier (**DOI**): https://doi.org/10.35882/jeeemi.v8i2.1524

while subplot (d) presents a consolidated view of their statistical performance metrics, including R^2, RMSE, and accuracy. A limitation of this study is that the baseline DFFNN trained using conventional backpropagation was not included, which may restrict isolation of the exact contribution of GWO to the feedforward architecture. Future work will incorporate this additional baseline and extend the experimental comparisons under broader training configurations.

F. Disccusion

Previous studies have demonstrated that ECG classification and prediction performance can be significantly influenced by the choice of feature representation and dataset characteristics, including signal segmentation strategies and subject diversity [29], [30], [31]. These factors play a crucial role in determining whether deep learning models or hybrid approaches achieve optimal performance. Based on the quantitative results n Table 4, the performance gap among the evaluated models is clear. The baseline LSTM achieved an average accuracy of 62.49% with an RMSE of 0.0356, indicating stable but limited predictive capability under the simplified training strategy where only the output layer was updated. The LSTM–GA model failed to improve upon this baseline, yielding accuracy values between 51.85% and 57.82% with a higher RMSE of approximately 0.0399, which suggests that the Genetic Algorithm optimization applied to a compact and fixed-gate LSTM structure did not provide sufficient representational enhancement. In contrast, the DFFNN-GWO model demonstrated a substantial numerical advantage, achieving an average R^2 of 0.9102, an accuracy of 91.02%, and a significantly lower RMSE of 0.0168. This numerical improvement indicates that global metaheuristic optimization via GWO is more effective at identifying robust weight configurations than gradient-based or hybrid recurrent learning when operating under small-subject ECG conditions.

When compared with previous studies, the findings of this work reveal an important contextual distinction. Prior ECG-related studies employing deep learning architectures such as CNN, LSTM, or CNN-LSTM hybrids have reported high prediction or classification accuracy when trained on large-scale benchmark datasets such as MIT-BIH or PhysioNet. For instance, CNN-LSTM-based ECG analysis and wavelet-based CNN approaches have demonstrated strong performance under extensive training data conditions. However, these approaches rely heavily on large datasets with substantial subject diversity. In contrast, the present study operates on a limited-subject elderly ECG dataset, where the number of participants is small despite the availability of sequential samples. Under this constraint, the superior performance of the DFFNN-GWO model indicates that metaheuristic-driven optimization can compensate for limited data diversity more effectively than gradient-based recurrent learning, particularly in small-data biomedical scenarios. [2], [3], [23], [24]. When compared with previous studies, the findings of this work highlight an important contextual distinction related to dataset scale and subject diversity. Recent ECG forecasting research using LSTM-based architectures has shown strong predictive capability when trained on large public datasets with many recordings and standardized acquisition conditions. For example, Zacarias et al. developed an LSTM forecasting system using ECG recordings from the MIT-BIH database and reported low error metrics under a deep recurrent configuration and extensive training data [24]. In general, studies built on PhysioNet/MIT-BIH-style data benefit from broader inter-subject variability and longer recordings, which can stabilize recurrent learning and reduce overfitting to subject-specific morphology. Therefore, performance trends reported in large-scale benchmark settings may not directly translate to limited-subject biomedical studies where the number of participants is small, despite having thousands of sequential samples.

Other related works have proposed hybrid signal decomposition and learning frameworks to improve ECG prediction robustness. For instance, Huang et al. introduced a hybrid ECG prediction method that integrates decomposition strategies with learning-based modeling to enhance predictive accuracy and support body-area-network scenarios [25]. These hybrid approaches typically exploit richer datasets and benefit from more diverse training patterns, which help the model learn invariant dynamics across subjects. In contrast, the present study focuses on a limited-subject elderly ECG dataset, where inter-subject diversity is inherently constrained. Under this condition, the superior performance of DFFNN-GWO suggests that metaheuristic-driven optimization can provide a more robust alternative to gradient-based recurrent learning, because it searches weight configurations globally and can remain effective even when the training distribution is narrow. This comparison reinforces that, in small-subject biomedical settings, optimization strategy and model simplicity may play a more decisive role than architectural depth in achieving reliable ECG forecasting.

Despite the promising results, several limitations of this study should be acknowledged. First, the ECG dataset was collected from a limited number of elderly participants, which restricts inter-subject variability and may affect the generalization of the models to broader populations. Second, the baseline LSTM employed a simplified training strategy with fixed internal gate parameters, which may limit its ability to fully capture complex temporal dependencies in ECG signals. Third, the study did not include a conventionally trained DFFNN using backpropagation, which restricts the isolation of the exact performance gain contributed solely by the Grey Wolf Optimizer. Finally, the evaluation was conducted with six experimental replications, and additional replications could further strengthen the statistical robustness of the findings.

The findings of this study have important practical implications for real-world ECG monitoring applications. The superior performance of the lightweight DFFNN-GWO model suggests that accurate ECG signal prediction can be achieved without relying on deep and computationally intensive architectures. This

Manuscript received 8 August 2025; Revised 20 February 2026; Accepted 20 March 2026; Available online 23 April 2026
Digital Object Identifier (DOI): https://doi.org/10.35882/jeeemi.v8i2.1524

characteristic makes the proposed approach particularly suitable for deployment in resource-constrained environments such as wearable ECG devices, portable health monitoring systems, and telemedicine platforms. By reducing computational complexity while maintaining high predictive accuracy, metaheuristic-optimized feedforward neural networks offer a viable solution for real-time cardiac monitoring and decision-support systems, especially in community-based or remote healthcare settings. The current evaluation is limited to in-sample one-step-ahead prediction and does not reflect true out-of-sample generalization. Therefore, the reported performance should be interpreted as an assessment of fitting capability rather than predictive generalization. Similar findings have been reported in recent studies where metaheuristic-driven models outperform conventional deep learning approaches under data constrained conditions [38], [39], [40]. These results suggest that optimization strategy can play a more dominant role than model complexity when dealing with limited and noisy biomedical datasets [41], [42].

IV. Conclusion

This study presents a comparative evaluation of single-stage and multi-stage metaheuristic optimization applied to DFFNN for ECG-based emotion classification under limited-subject conditions. The results indicate that multi-stage optimization (GA+GWO) provides improved training stability and achieves the lowest MSE among the models. However, the improvement in generalization performance remains limited, as reflected by modest test accuracy. These findings suggest that optimization strategy plays a significant role in stabilizing neural network training in small-data biomedical applications. Nevertheless, the conclusions are constrained by the experimental setup, particularly the limited dataset size and absence of subject-wise validation. Future work will focus on expanding the dataset, implementing subject-independent validation, incorporating stronger baseline models, and improving preprocessing techniques to enhance generalization capability. These findings should be interpreted as preliminary and context-specific, requiring further validation on larger and more diverse datasets before broader conclusions can be drawn.

Acknowledgment

The authors would like to express their sincere gratitude to the Department of Electrical Engineering, Universitas 17 Agustus 1945 Surabaya, for the support and facilities provided throughout this research. The authors also extend their appreciation to all participants (elderly people from GKJW Waru) who voluntarily contributed to the ECG data collection process. Their cooperation and willingness made this study possible.

Funding

This research received no specific grant from any funding agency in the public, commercial, or not-for-profit sectors.

Data Availability

The datasets generated and analyzed during the current study are not publicly available due to privacy and ethical restrictions involving human participants, but are available from the corresponding author on reasonable request.

Author Contribution

Giovanni Dimas Prenata conceptualized and designed the study, developed the models, conducted data analysis, and wrote the manuscript. Ahmad Ridho'i contributed to data collection, preprocessing, and experimental implementation. Mohd Rizal Arshad provided methodological guidance, contributed to the interpretation of results, and reviewed the manuscript. All authors reviewed and approved the final version of the manuscript and agreed to be accountable for all aspects of the work.

Declarations

Ethical Approval

This study was conducted in accordance with ethical standards for research involving human participants. Ethical approval was obtained from the Institutional Review Board (IRB) of Universitas 17 Agustus 1945 Surabaya. All procedures complied with relevant guidelines and regulations for biomedical research involving human subjects.

Consent for Publication Participants.

Informed consent for publication was obtained from all participants involved in the study. All data were anonymized to ensure participant confidentiality.

Competing Interests

The authors declare that they have no competing interests.

References

[1] S. Hochreiter and J. Schmidhuber, "Long Short-Term Memory," *Neural Comput.*, vol. 9, no. 8, pp. 1735–1780, 1997, doi: 10.1162/neco.1997.9.8.1735.

[2] Q. Xiao *et al.*, "Deep Learning-Based ECG Arrhythmia Classification: A Systematic Review," *Appl. Sci.*, vol. 13, no. 8, 2023, doi: 10.3390/app13084964.

[3] G. D. Clifford, F. Azuaje, and P. E. McSharry, "Advanced Methods and Tools for ECG Data Analysis," *Adv. Methods Tools ECG Data Anal.*, pp. 1–400, 2006.

[4] G. N. Chandrika, A. Mitra, V. Satheeswaran, R. Chowdhury, P. Kumar, and E. Glory, "Deep Learning Based Classification of ECG Signals to Detect Heart Diseases Using RNN and LSTM Mechanism," *J. Electron. Electromed. Eng. Med. Informatics*, vol. 6, no. 4, pp. 332–342, 2024, doi: 10.35882/jeeemi.v6i4.496.

[5] H. M. Rai and A. Trivedi, "ECG signal classification using wavelet transform and Back Propagation Neural Network," *CODEC 2012 - 5th Int. Conf. Comput. Devices Commun.*, vol. 3, pp. 212–215,

Manuscript received 8 August 2025; Revised 20 February 2026; Accepted 20 March 2026; Available online 23 April 2026
Digital Object Identifier (**DOI**): https://doi.org/10.35882/jeeemi.v8i2.1524

2012, doi: 10.1109/CODEC.2012.6509183.

[6] H.-C. CHEN and K. HIRASAWA, "Adaptation in Natural and Artificial Systems: An Introductory Analysis with Applications to Biology, Control and Artificial Intelligence Adaptation in Natural and Artificial Systems: An Introductory Analysis with Applications to Biology, Control and Artif," 2006.

[7] S. Mirjalili, S. M. Mirjalili, and A. Lewis, "Grey Wolf Optimizer," *Adv. Eng. Softw.*, vol. 69, pp. 46–61, 2014, doi: 10.1016/j.advengsoft.2013.12.007.

[8] P. Srinivasu and P. S. Avadhani, "Genetic algorithm based weight extraction algorithm for artificial neural network classifier in intrusion detection," *Procedia Eng.*, vol. 38, pp. 144–153, 2012, doi: 10.1016/j.proeng.2012.06.021.

[9] B. Rabhi, H. Dhahri, A. M. Alimi, and F. A. Alturki, "Grey wolf optimizer for training elman neural network," *Adv. Intell. Syst. Comput.*, vol. 552, pp. 380–390, 2017, doi: 10.1007/978-3-319-52941-7_38.

[10] B. Surawicz, R. Childers, B. J. Deal, and L. S. Gettes, "AHA/ACCF/HRS Recommendations for the Standardization and Interpretation of the Electrocardiogram. Part III: Intraventricular Conduction Disturbances A Scientific Statement From the American Heart Association Electrocardiography and Arrhythmias Committee, ," *J. Am. Coll. Cardiol.*, vol. 53, no. 11, pp. 976–981, 2009, doi: 10.1016/j.jacc.2008.12.013.

[11] B. J. Drew *et al.*, "Practice standards for electrocardiographic monitoring in hospital settings: An American Heart Association scientific statement from the councils on cardiovascular nursing, clinical cardiology, and cardiovascular disease in the young," *Circulation*, vol. 110, no. 17, pp. 2721–2746, 2004, doi: 10.1161/01.CIR.0000145144.56673.59.

[12] McSharry, P. E., Clifford, G. D., Tarassenko, L., and Smith, L. A., "A Dynamical Model for Generating Synthetic Electrocardiogram Signals," *IEEE Transactions on Biomedical Engineering*, vol. 50, no. 3, pp. 289–294, 2003. doi: 10.1109/TBME.2003.808805.

[13] I. Goodfellow, "Front Matter," *Linear Algebr.*, pp. i–ii, 2014, doi: 10.1016/b978-0-12-391420-0.09987-x.

[14] O. Faust, Y. Hagiwara, T. J. Hong, O. S. Lih, and U. R. Acharya, "Deep learning for healthcare applications based on physiological signals: A review," *Comput. Methods Programs Biomed.*, vol. 161, no. April, pp. 1–13, 2018, doi: 10.1016/j.cmpb.2018.04.005.

[15] M. M. A. Rahhal, Y. Bazi, H. Alhichri, N. Alajlan, F. Melgani, and R. R. Yager, "Deep learning approach for active classification of electrocardiogram signals," *Inf. Sci. (Ny).*, vol. 345, pp. 340–354, 2016, doi: 10.1016/j.ins.2016.01.082.

[16] M. S. Shaikh *et al.*, *An intelligent hybrid grey wolf-particle swarm optimizer for optimization in complex engineering design problem*, vol. 15, no. 1. 2025. doi: 10.1038/s41598-025-02154-0.

[17] M. Mitchell, "An Introduction to Genetic Algorithms," *An Introd. to Genet. Algorithms*, pp. 115–123, 1996, doi: 10.7551/mitpress/3927.001.0001.

[18] P. A. Thompson, "An MSE statistic for comparing forecast accuracy across series," *Int. J. Forecast.*, vol. 6, no. 2, pp. 219–227, 1990, doi: 10.1016/0169-2070(90)90007-X.

[19] M. Srinivas and L. M. Patnaik, "Genetic Algorithms: A Survey," *Computer (Long. Beach. Calif).*, vol. 27, no. 6, pp. 17–26, 1994, doi: 10.1109/2.294849.

[20] S. Mirjalili, "How effective is the Grey Wolf optimizer in training multi-layer perceptrons," *Appl. Intell.*, vol. 43, no. 1, pp. 150–161, 2015, doi: 10.1007/s10489-014-0645-7.

[21] A. H. Gandomi, X. S. Yang, S. Talatahari, and A. H. Alavi, *Metaheuristic Algorithms in Modeling and Optimization*, no. May 2017. 2013. doi: 10.1016/B978-0-12-398364-0.00001-2.

[22] G. D. Prenata, E. S. Pane, A. D. Wibawa, and M. H. Purnomo, "Analysis of negative emotion using HRV based ECG signal of elder people," *Proc. - 2017 2nd Int. Conf. Inf. Technol. Inf. Syst. Electr. Eng. ICITISEE 2017*, vol. 2018–Janua, pp. 444–449, 2017, doi: 10.1109/ICITISEE.2017.8285547.

[23] P. S. Addison, "Wavelet transforms and the ECG: A review," *Physiol. Meas.*, vol. 26, no. 5, 2005, doi: 10.1088/0967-3334/26/5/R01.

[24] H. Zacarias, J. A. L. Marques, V. Felizardo, M. Pourvahab, and N. M. Garcia, "ECG Forecasting System Based on Long Short-Term Memory," *Bioengineering*, vol. 11, no. 1, pp. 1–17, 2024, doi: 10.3390/bioengineering11010089.

[25] F. Huang, T. Qin, L. Wang, and H. Wan, "Hybrid Prediction Method for ECG Signals Based on VMD, PSR, and RBF Neural Network," *Biomed Res. Int.*, vol. 2021, 2021, doi: 10.1155/2021/6624298.

[26] Pressman, S. D., and Cohen, S., "Does positive affect influence health?," *Psychological Bulletin*, vol. 131, no. 6, pp. 925–971, 2005. doi: 10.1037/0033-2909.131.6.925.

[27] Gross, J. J., "Emotion Regulation: Conceptual Foundations," *in Handbook of Emotion Regulation*, New York: Guilford Press, 2007, pp. 3–24/27.

[28] Kreibig, S. D., "Autonomic nervous system activity in emotion: A review," *Biological Psychology*, vol. 84, no. 3, pp. 394–421, 2010. doi: 10.1016/j.biopsycho.2010.03.010.

[29] Naseer, N., and Nazeer, H., "Classification of normal and abnormal ECG signals based on their PQRST intervals," in *Proceedings of the 2017 International Conference on Mechanical, System and Control Engineering (ICMSC), 2017*, pp. 388–391. doi: 10.1109/ICMSC.2017.7959507.

[30] Gualsaqui Miranda, M. V., Vizcaíno Espinosa, I. P., and Flores Calero, M. J., "ECG signal features extraction," in *2016 IEEE ANDESCON*, 2016. doi: 10.1109/ETCM.2016.7750859.

[31] Lim, J., Han, D., Nejad, M. P. S., and Chon, K. H., "ECG classification via integration of adaptive beat

Manuscript received 8 August 2025; Revised 20 February 2026; Accepted 20 March 2026; Available online 23 April 2026
Digital Object Identifier (**DOI**): https://doi.org/10.35882/jeeemi.v8i2.1524

segmentation and relative heart rate with deep learning networks," *Computers in Biology and Medicine*, vol. 181, Art. no. 109062, Oct. 2024. doi: 10.1016/j.compbiomed.2024.109062.

[32] Sharma, M., and Sharma, A., "HRV: A powerful tool in medical diagnosis," in *Handbook of Research on Emerging Trends in Medical Informatics*, IGI Global, 2020. doi: 10.4018/978-1-5225-9787-2.ch013.

[33] Guyton, A. C., and Hall, J. E., *Textbook of Medical Physiology*, 11th ed., Philadelphia, PA: Elsevier Saunders, 2006.

[34] Alam, A., Urooj, S., and Ansari, A. Q., "Human emotion recognition models using machine learning techniques," in *2023 International Conference on Recent Advances in Electrical, Electronics and Digital Healthcare Technologies (REEDCON)*, 2023, pp. 329–334. doi: 10.1109/REEDCON57544.2023.10151406.

[35] Zhang, L., and Wang, J., "Design for emotion classification and retrieval of video based on user experience," in *Proceedings of the 2011 International Conference on Electronics, Communications and Control (ICECC)*, 2011, pp. 205–211. doi: 10.1109/ICECC.2011.6066429.

[36] Kim, J., and André, E., "Emotion recognition based on physiological changes in music listening," *IEEE Transactions on Pattern Analysis and Machine Intelligence*, vol. 30, no. 12, pp. 2067–2083, 2008. doi: 10.1109/TPAMI.2008.26.

[37] Xu, Y., and Liu, G., "A method of emotion recognition based on ECG signal," in *Proceedings of the International Conference on Computational Intelligence and Natural Computing (CINC)*, 2009. doi: 10.1109/CINC.2009.102.

[38] Shu, L., Xie, J., Yang, M., Li, Z., Li, Z., Liao, D., Xu, X., and Yang, X., "A review of emotion recognition using physiological signals," *Sensors*, vol. 18, no. 7, Art. no. 2074, 2018. doi: 10.3390/s18072074.

[39] Fikri, M. R., Soesanti, I., and Nugroho, H. A., "ECG signal classification review," *International Journal of Information Technology and Electrical Engineering (IJITEE)*, vol. 5, no. 1, pp. 15–20, 2021. doi: 10.22146/ijitee.60295.

[40] He, L., Hou, W.-S., Zhen, X., and Peng, C. L., "Recognition of ECG patterns using artificial neural network," in *Proceedings of the International Symposium on Intelligent Data Analysis (ISDA)*, 2006, pp. 477–481. doi: 10.1109/ISDA.2006.253883.

[41] Guo, H.-W., Huang, Y.-S., Lin, C.-H., Chien, J.-C., Haraikawa, K., and Shieh, J.-S., "Heart rate variability signal features for emotion recognition by using principal component analysis and support vector machine," in *2016 IEEE 16th International Conference on Bioinformatics and Bioengineering (BIBE)*, 2016, pp. 274–277. doi: 10.1109/BIBE.2016.40.

[42] Faust, O., Hong, W., Loh, H. W., Xu, S., Tan, R. S., Chakraborty, S., Barua, P. D., Molinari, F., and Acharya, U. R., "Heart rate variability for medical decision support systems: A review," *Computers in Biology and Medicine*, vol. 145, Art. no. 105407, 2022. doi: 10.1016/j.compbiomed.2022.105407.

Author Biography

Giovanni Dimas Prenata

He received his B.Eng. in Electrical Engineering (Power Systems) from Petra Christian University, Surabaya, in 2009. His undergraduate research focused on energy management and efficiency optimization. He obtained his M.Eng. in Electrical Engineering (Telematics) from Institut Teknologi Sepuluh Nopember (ITS), Surabaya, in 2018, where his thesis addressed electrocardiogram (ECG) signal classification using a Support Vector Machine (SVM) to identify negative emotional responses in elderly subjects. His research interests include artificial intelligence, biomedical signal processing, and computational modeling, with an emphasis on developing C++-based intelligent algorithms for applications in energy and healthcare systems.

Ahmad Ridho'i

He received his B.Eng. in Electrical Engineering (Electronics) from Universitas 17 Agustus 1945 Surabaya in 1995, where his undergraduate research focused on developing a speech assistance device using an IBM-based personal computer. He obtained his M.Eng. in Electrical Engineering (Electrotechnics) from the Bandung Institute of Technology (ITB) in 2000, with research on intelligent control systems for optimizing elevator service queues. His research interests include disaster mitigation and early warning systems, particularly in the context of Indonesia's vulnerability to natural disasters. His work focuses on developing community-based monitoring technologies to reduce risks and enhance disaster preparedness.

Manuscript received 8 August 2025; Revised 20 February 2026; Accepted 20 March 2026; Available online 23 April 2026
Digital Object Identifier (**DOI**): https://doi.org/10.35882/jeeemi.v8i2.1524